photonics

IMPACT FACTOR 2.536

CITESCORE 2.3

Article

Antibunching Effects in the Hybrid Cavity–Bose–Einstein Condensates System

Zhen Li and Wangjun Lu

MDPI

https://doi.org/10.3390/photonics10020123

photonics

MDPI

Article

Antibunching Effects in the Hybrid Cavity–Bose–Einstein Condensates System

Zhen Li [1,*] and Wangjun Lu [2,3]

[1] Department of Physics, Shaoyang University, Shaoyang 422099, China
[2] Department of Physics, Zhejiang Institute of Modern Physics, Zhejiang University, Hangzhou 310027, China
[3] Department of Maths and Physics, Hunan Institute of Engineering, Xiangtan 411104, China
* Correspondence: zhenli@hnsyu.edu.cn

Abstract: We theoretically study the model of a hybrid cavity–Bose–Einstein condensates (BEC) system that consists of a two-level impurity atom coupled to a cavity–BEC system with radiation pressure coupling, where the system is weakly driven by a monochromatic laser field. The steady-states behavior of the entire system is researched in the framework of the impurity–cavity coupling dispersive limit. We find that the multiple types of photon steady-state antibunching effects can be obtained when only the dissipation of the cavity is included. Moreover, the strength and frequency range of conventional steady-state antibunching effects of the cavity can be significantly modified by the impurity atom and intrinsic non-linearity of BEC. This result shows that our study can provide a method to tune the antibunching effects of the cavity field. In addition, the non-standard photon blockade or superbunching effect with the suppression of two-photon correlation and enhancement of three-photon correlation can be realized. The frequency range of the superbunching effect also can be changed by the impurity atom and intrinsic non-linearity of BEC. Therefore, our study shows many quantum statistical characteristics in a hybrid cavity–BEC quantum system and its manipulation.

Keywords: antibunching effects; superbunching effect; cavity–Bose–Einstein condensates; impurity; nonlinearity

Citation: Li, Z.; Lu, W. Antibunching Effects in the Hybrid Cavity–Bose–Einstein Condensates System. *Photonics* **2023**, *10*, 123. https://doi.org/10.3390/photonics10020123

Received: 21 December 2022
Revised: 17 January 2023
Accepted: 21 January 2023
Published: 26 January 2023

1. Introduction

In quantum optics and quantum information processing, the research of photon manipulation has been an important issue [1–8]. It is believed that photon antibunching [9–11] is the key requirement for realizing the generation and manipulation of photons. Such photon antibunching effects could generate photon streams [12,13], leading to many applications in non-linear quantum optics, such as ideal single photon sources [14,15] or entangled photon sources [16–18]. So, we need to research the manipulation of photon antibunching effects. Antibunching of photons (photon blockade) refers to the effects in which photons generated in a driven non-linear system can block the generation of more photons in the system. Thus, the prerequisite for realizing these conventional photon antibunching effects in quantum systems is the presence of strong non-linearities in the system. So far, much effort has been devoted to the antibunching effects of photons in various quantum systems, e.g., circuit QED [19,20], cavity QED [21,22], and bare optomechanical systems [23,24]. However, the manipulation of multiple types of photon antibunching effects has not been studied in the cavity–Bose–Einstein condensates (BEC) system.

The radiation pressure coupling between atom and light in the cavity–BEC system can be realized due to the ultracold atoms being collectively coupled to the same optical mode [25–27]. One of the advantages of this collective mode which plays the role of the vibrational mode of a moving mirror or a membrane is coupling to the radiation pressure of the cavity can be increased to strong coupling by increasing the number of atoms [28,29]. On the other hand, there are other different kinds of non-linearities in cavity–BEC systems

with radiation pressure coupling. One of the most significant non-linear effects within ultracold atoms is due to the atom–atom interaction, which can result in the squeezing of the matter field of the ultracold atoms [30,31]. Both kinds of these non-linearities have a great influence on the optical properties of the cavity output optical field [32–34]. Thus, the cavity–BEC system provides an ideal platform for the generation and manipulation of photon antibunching effects.

Motivated by the recent theoretical and experimental progress of impurity-doped-BEC systems due to numerous applications in probing strongly correlated quantum many-body states [35,36], quantum state engineering [37–45], quantum resource manipulation [46–49], quantum metrology [50–53], and some new hybrid atom–cavity quantum systems [54–56]. In this paper, we propose a hybrid cavity–BEC quantum system with radiation pressure coupling. This hybrid cavity–BEC system is composed of a two-level impurity atom, a cigar-shaped BEC, and a Fabry–Perot cavity, where the impurity atom is immersed in the cigar-shaped BEC to form the impurity-doped BEC systems, which are trapped inside a Fabry–Perot cavity. This hybrid cavity–BEC system is an integration of the impurity-doped BEC systems and the cavity–BEC systems with radiation pressure coupling. The approximate analytical expression of the steady-state second-order correlation (SOC) and third-order correlation (TOC) function for the cavity field is obtained. Then, we propose a scheme to manipulate the multiple types of optical antibunching effects in the hybrid cavity–BEC quantum system via a two-level impurity or intrinsic non-linearity of BEC.

This paper is organized as follows: in Section 2, we first describe the hybrid cavity–BEC quantum system in the dispersive limit (i.e., far-off resonance). Moreover, the effective Hamiltonian for our hybrid quantum system under the Bogoliubov approximation is proposed. Secondly, we introduce the diagonalization process of the hybrid system Hamiltonian through two steps and provide the eigenvalues and eigenstates of the hybrid system. In Section 3, we use an approximation method to obtain the analytical expression of the zero-time-delay normalized SOC and TOC function of the cavity field for our hybrid system in the weak pumping limit. Then, according to the SOC and TOC function, the effects of impurity and BEC on the cavity field antibunching effects are analyzed. Finally, we give conclusions of our work in Section 4.

2. Physical Model and Solution

The hybrid cavity–Bose–Einstein condensate (BEC) quantum system is composed of a two-level impurity atom and cavity–BEC quantum system with radiation pressure coupling. As schematically shown in Figure 1, the impurity atom is frozen in place [57,58]. The relevant internal level structure for the impurity atom is given by the atomic ground state $|g\rangle$ and the excited state $|e\rangle$, which form a two-level system with transition frequency ω_i. This impurity atom will interact both with BEC and the cavity. Next, we will introduce the effective Hamiltonian of the system and provide the corresponding eigenstates and eigenvalues.

2.1. System Hamiltonian

The cavity–BEC quantum system consists of a cigar-shaped BEC of N two-level atoms with transition frequency ω_b and mass m_b inside a Fabry–Pérot optical cavity with length L. Thus, the Hamiltonian of the hybrid cavity–BEC quantum system with radiation pressure coupling reads

$$H = H_{CB} + H_{iB} + H_{iC} + H_d. \tag{1}$$

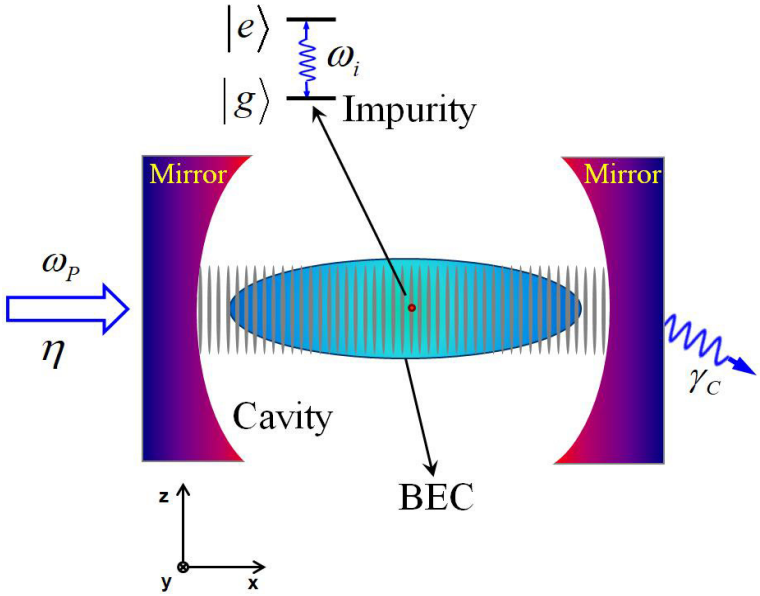

Figure 1. Schematic diagram of the cavity–BEC (cigar-shaped) system with a two-level impurity.

The BEC is confined in a cylindrically symmetric trap with a transverse trapping frequency $\omega_\perp$ and the longitudinal confinement along the x direction is negligible [59]. In this way, the dynamics of the system can be described within an effective one-dimensional model by quantizing the atomic motional degree of freedom along just the x axis. The cavity is driven at rate $\eta = \sqrt{2P\gamma_a/\omega_p}$ through one of the fixed mirrors by a laser with frequency ω_p and wave number $k = \omega_p/c$, where P is the laser power and γ_a is the decay rate of the cavity. In our situation, the excited electronic state of the atoms can be adiabatically eliminated, and the atomic spontaneous emission can be neglected when the detuning $\Delta_b = \omega_p - \omega_b$ is orders of magnitude larger than the atomic linewidth [60]. We set $\hbar = 1$ throughout the paper. In the frame rotating at the pump frequency ω_p, the Hamiltonian of the cavity–BEC quantum system with radiation pressure coupling [60,61] is

$$H_{CB} + H_d = \Delta_a a^\dagger a + \int_{-L/2}^{L/2} d\mathbf{x}\Psi^\dagger(\mathbf{x})\left[-\frac{1}{2m}\nabla^2 + V(\mathbf{x}) + \frac{U_s}{2}\Psi^\dagger(\mathbf{x})\Psi(\mathbf{x})\right]\Psi(\mathbf{x}) + \eta(a + a^\dagger), \tag{2}$$

where a ($a^\dagger$) and $\Psi(\mathbf{x})$ $\left(\Psi^\dagger(\mathbf{x})\right)$ are, respectively, the annihilation (creation) operations of the cavity and atomic field. $\Delta_a = \omega_a - \omega_p$ is the detuning between the cavity and pump laser. $V(\mathbf{x}) = U_0\cos^2(k\mathbf{x})a^\dagger a$ represents the atomic back action on the field. $U_0 = g_0^2/\Delta_b$ is the optical lattice barrier height for per photon, where g_0 is the vacuum Rabi frequency. $U_s = 4\pi a_s/m_b L_0^2$ is the non-linear interaction within the BEC, where a_s is the two-body s-wave scattering length [62–64], and L_0 is the waist radius of the optical potential. $H_d = \eta(a + a^\dagger)$ describes the driving process.

The coupling between the BEC and two-level impurity occurs in the form of a density–density interaction [36,53,65]. The Hamiltonian describes

$$H_{iB} = \frac{\omega_i}{2}\sigma_z + \lambda|e\rangle\langle e|\int_{-L/2}^{L/2} d\mathbf{x}|\phi(\mathbf{x})|^2\Psi^\dagger(\mathbf{x})\Psi(\mathbf{x}), \tag{3}$$

where λ is the interaction strength, and $\phi(\mathbf{x})$ is the wavefunction of a two-level impurity atom in the x direction. The interaction strength between impurity and BEC is proportional to the s-wave scattering length, which can be greatly increased by tuning an external magnetic field near a Feshbach resonance [62] so that the interaction strength is greatly enhanced, and does not change their population. This coherent collision will change the relative phase of the two internal states. In addition, we assume that coherent collisions between the impurity atom and the BEC will not further excite the motional state of the single atom [36,65].

The impurity is considered a two-level quantum system in our situation (i.e., qubit). Under the rotating wave approximation, the interaction Hamiltonian between a qubit and single-mode cavity field is given by

$$H_{iC} = g(a^{\dagger}\sigma_{-} + a\sigma_{+}), \tag{4}$$

where g is the coupling strength, and the Pauli operator $\sigma_{+}(\sigma_{-})$ is defined by $\sigma_{+} = |e\rangle\langle g|$ $(\sigma_{-} = |g\rangle\langle e|)$. We assume the detuning $\omega_i - \omega_a$ is large enough such that direct atomic transitions do not occur but where, nevertheless, dispersive interactions between a qubit and single-mode cavity field do occur [66–69]. The effective qubit–cavity field interaction Hamiltonian in the case of large detuning is given by

$$H'_{iC} = \frac{g^2}{\omega_i - \omega_a}\left(\sigma_{+}\sigma_{-} + a^{\dagger}a\sigma_z\right), \tag{5}$$

where the term $g^2\sigma_{+}\sigma_{-}/(\omega_i - \omega_a)$, present even in the absence of photons, is a kind of cavity induced qubit Kerr non-linearity effect giving rise to an energy shift on the bare excited state $|e\rangle$ of qubit. This cavity–qubit dispersion interaction sometimes as a primary means of performing specific quantum work, and sometimes behaves as a kind of noise [70–72].

In the weakly interacting regime, the intracavity photon number is so low that the condition $U_0\langle a^{\dagger}a\rangle \leq 10\omega_R$ is satisfied, where $\omega_R = k^2/2m_b$ is the recoil frequency of the condensate atoms. We can restrict ourselves to the first two symmetric momentum side modes with momenta $\pm 2k$, which are excited by the atom–cavity field interaction [73]. In this way, because of the parity conservation and considering the Bogoliubov approximation, the atomic annihilation (creation) field operators $\Psi(\mathbf{x})$ $\left(\Psi^{\dagger}(\mathbf{x})\right)$ of the BEC can be expanded as the following single-mode quantum fields

$$\Psi(\mathbf{x}) = \sqrt{\frac{N}{L}} + \sqrt{\frac{2}{L}}\cos(2k\mathbf{x})b, \tag{6}$$

$$\Psi^{\dagger}(\mathbf{x}) = \sqrt{\frac{N}{L}} + \sqrt{\frac{2}{L}}\cos(2k\mathbf{x})b^{\dagger}, \tag{7}$$

where the term $\sqrt{N/L}$ is the constant number which is considered condensate mode. The annihilation (creation) operator b $(b^{\dagger})$ in the second term is the Bogoliubov mode of BEC, which corresponds to the quantum fluctuations of the atomic field about the classical condensate mode [73]. By substituting the atomic field operator of Equation (6) and Equation (7) into Equation (2), the Hamiltonian of the cavity–BEC quantum system with radiation pressure coupling has the following form

$$H'_{CB} = \delta_a a^{\dagger}a + \Omega_b b^{\dagger}b + \frac{1}{4}\lambda_s(b^2 + b^{\dagger 2}) + \frac{\sqrt{2}}{2}\lambda_{CB}a^{\dagger}a(b + b^{\dagger}) + \lambda_{ck}a^{\dagger}ab^{\dagger}b + \lambda_{sk}b^{\dagger 2}b^2, \tag{8}$$

where $\delta_a = NU_0/2 + \Delta_a$ is the Stark-shifted cavity frequency. This frequency shift is induced by the interaction of cavity–BEC and related to the number of atoms in the condensate. $\Omega_b = 4\omega_R + \lambda_s$ is the frequency of the Bogoliubov mode, where $\lambda_s = 8\pi a_s N/Lm_bL_0$ is the s-wave scattering frequency of the atomic collisions. $\lambda_{CB} = \sqrt{N}U_0/2$ is the radiation pressure coupling between the Bogoliubov mode of BEC and the cavity mode. $\lambda_{ck} = U_0/2$ is the cross-Kerr non-linearity interaction between the BEC and cavity modes. $\lambda_{sk} = 3\pi a_s/Lm_bL_0^2 = 3\lambda_s/8N$ is the intrinsic-Kerr non-linearity interaction in BEC.

One can easily find that the ratio of the radiation pressure coupling λ_{CB} to cross-Kerr interaction λ_{ck} is of the order of $\sqrt{N}$ and atom–atom interactions interaction λ_s to intrinsic-Kerr coupling λ_{sk} is of the order of N. Thus, the cross-Kerr term and intrinsic-Kerr term are negligible in comparison to the radiation pressure and atomic collisions for very large

values of N. The Hamiltonian of the cavity–BEC quantum system with radiation pressure coupling reduces to

$$H''_{CB} = \delta_a a^\dagger a + \Omega_b b^\dagger b + \frac{1}{4}\lambda_s(b^2 + b^{\dagger 2}) + \frac{\sqrt{2}}{2}\lambda_{CB} a^\dagger a(b + b^\dagger). \tag{9}$$

Similarly, by substituting Equations (6) and (7) into Equation (3), the Hamiltonian of the two-level impurity-doped-BEC quantum system reads

$$H'_{iB} = \frac{\omega_i}{2}\sigma_z + \omega_{iB}|e\rangle\langle e| + \lambda_{iB}|e\rangle\langle e|\left(b + b^\dagger\right) + \sqrt{2}\lambda'_{iB}|e\rangle\langle e|b^\dagger b, \tag{10}$$

where $\omega_{iB} = \lambda N/L$ is a frequency shift on the bare excited qubit state $|e\rangle$. This frequency shift is induced by density–density interaction between the excited state of impurity and classical condensate mode. $\lambda_{iB} = \lambda\sqrt{2N}\int_{-L/2}^{L/2} d\mathbf{x}|\phi(\mathbf{x})|^2\cos(2k\mathbf{x})/L$ and $\lambda'_{iB} = \sqrt{2}\lambda\int_{-L/2}^{L/2} d\mathbf{x}|\phi(\mathbf{x})|^2\cos^2(2k\mathbf{x})/L$ are, respectively, linear coupling and coherent collisions interaction between the excited state of impurity and Bogoliubov mode of BEC (i.e., quantum fluctuations of the atomic field about the classical condensate mode $\sqrt{N/L}$). The ratio of the linear coupling λ_{iB} to coherent collision interaction λ'_{iB} is of the order of $\sqrt{N}$. So, the coherent collisions interaction term can be removed when N is large enough. The Hamiltonian of the two-level impurity-doped-BEC quantum system has the following form

$$H''_{iB} = \frac{\omega_i + \omega_{iB}}{2}\sigma_z + \frac{\lambda_{iB}}{2}(\sigma_z + 1)\left(b + b^\dagger\right), \tag{11}$$

where operator σ_z is defined by $\sigma_z = |e\rangle\langle e| - |g\rangle\langle g|$.

Combining the Equations (5), (9), and (11), the total Hamiltonian of the three-body hybrid cavity–BEC quantum system takes the form

$$\begin{aligned} H_{tot} &= \delta_a a^\dagger a + \Omega_b b^\dagger b + \frac{1}{4}\lambda_s(b^2 + b^{\dagger 2}) + \frac{\sqrt{2}}{2}\lambda_{CB} a^\dagger a(b + b^\dagger) \\ &\quad + \frac{g^2}{\omega_i - \omega_a}\left(\sigma_+\sigma_- + a^\dagger a\sigma_z\right) + \frac{\omega_i + \omega_{iB}}{2}\sigma_z + \frac{\lambda_{iB}}{2}(\sigma_z + 1)\left(b + b^\dagger\right) \\ &= \delta_a a^\dagger a + \Omega_b b^\dagger b + \frac{\omega'_i}{2}\sigma_z + \lambda_{iC} a^\dagger a\sigma_z + \frac{1}{4}\lambda_s(b^2 + b^{\dagger 2}) \\ &\quad + \frac{1}{2}\left[\sqrt{2}\lambda_{CB} a^\dagger a + \lambda_{iB}(\sigma_z + 1)\right](b + b^\dagger) + \frac{g^2}{2(\omega_i - \omega_a)}, \end{aligned} \tag{12}$$

where $\omega'_i = g^2/(\omega_i - \omega_a) + \omega_i + \omega_{iB}$ is the effective energy gap between the ground state and the excited state of a two-level impurity atom. $\lambda_{iC} = g^2/(\omega_i - \omega_a)$ is the dispersive interaction strength between the two-level impurity and the single-mode cavity field. In the discussion that follows, we will diagonalize the Hamiltonian H_{tot} in two steps, and the last constant term will be neglected, which has no effect on the dynamics of the system. One can see Appendix A for diagonalization details. The diagonal Hamiltonian H''_{tot} takes the form

$$H''_{tot} = \delta_a a^\dagger a + \Omega'_b b^\dagger b + \frac{\omega'_i}{2}\sigma_z + \lambda_{iC} a^\dagger a\sigma_z - \left(\Omega_b + \frac{1}{2}\lambda_s\right)\alpha^2(a^\dagger a)^2. \tag{13}$$

2.2. The Eigenvalues and Eigenstates of the System

Using the displacement and squeezing unitary transformation (i.e., Equations (A1) and (A7)), the Hamiltonian of the system will take a diagonal form as follow:

$$H''_{tot} = S(\zeta)D(\alpha a^\dagger a)H_{tot}D^\dagger(\alpha a^\dagger a)S^\dagger(\zeta), \tag{14}$$

which is a diagonal Hamiltonian with the following eigenvalues and eigenstates

$$E_{n,m,e} = \delta_a n + \Omega_b' m + \frac{\omega_i'}{2} + \lambda_{iC} n - \frac{\left(\lambda_{CB} n + \sqrt{2}\lambda_{iB}\right)^2}{2\Omega_b + \lambda_s}, \tag{15}$$

$$E_{n,m,g} = \delta_a n + \Omega_b' m - \frac{\omega_i'}{2} - \lambda_{iC} n - \frac{(\lambda_{CB} n)^2}{2\Omega_b + \lambda_s}, \tag{16}$$

$$|\psi\rangle_{n,m,e} = |n\rangle \otimes |m\rangle \otimes |e\rangle, \tag{17}$$

$$|\psi\rangle_{n,m,g} = |n\rangle \otimes |m\rangle \otimes |g\rangle, \tag{18}$$

where $|n\rangle$ and $|m\rangle$, respectively, denote as the harmonic-oscillator number states of the cavity and the Bogoliubov mode. Then the eigensystem of the Hamiltonian H_{tot} can be obtained by

$$\begin{aligned} H_{tot}''|n\rangle|m\rangle|e(g)\rangle &= E_{n,m,e(g)}|n\rangle|m\rangle|e(g)\rangle, \\ H_{tot} D^\dagger(\alpha a^\dagger a) S^\dagger(\zeta)|n\rangle|m\rangle|e(g)\rangle &= E_{n,m,e(g)} D^\dagger(\alpha a^\dagger a) S^\dagger(\zeta)|n\rangle|m\rangle|e(g)\rangle, \\ H_{tot}|n\rangle|\tilde{m}(n)\rangle_{e(g)}|e(g)\rangle &= E_{n,m,e(g)}|n\rangle|\tilde{m}(n)\rangle_{e(g)}|e(g)\rangle, \end{aligned} \tag{19}$$

where the n-photon displacement squeezing number states in Equation (19) are defined by

$$|\tilde{m}(n)\rangle_{e(g)} = D^\dagger(\alpha_{e(g)} a^\dagger a) S^\dagger(\zeta)|m\rangle. \tag{20}$$

Thus, a general state of the system can be expressed as

$$|\varphi(t)\rangle = \sum_{n=0}^{\infty}\sum_{m=0}^{\infty} C_{n,m,e}(t)|n\rangle|\tilde{m}(n)\rangle_e|e\rangle + \sum_{n=0}^{\infty}\sum_{m=0}^{\infty} C_{n,m,g}(t)|n\rangle|\tilde{m}(n)\rangle_g|g\rangle. \tag{21}$$

3. Anti-Bunching Effect in the Cavity

To investigate the manipulation of the single-photon blockade, two-photon blockade and non-standard photon blockade, we will use an approximation method to analytically calculate the zero-time-delay normalized second-order correlation (SOC) and third-order correlation (TOC) function of the cavity photons.

3.1. Approximate Analytical Results

In our situation, when the hybrid cavity–BEC quantum system is driven by an external laser, there will also be a certain amount of dissipation. Then, we phenomenologically add an anti-Hermitian term to Hamiltonian Equation (12) to describe the dissipation of the cavity photons and neglect the BEC and the impurity decoherence when the rate of impurity and Bogoliubov mode dissipation satisfy $\gamma_c \gg \gamma_b \gg \gamma_i$ (i.e., γ_b and γ_i are, respectively, Bogoliubov mode and impurity dissipation). Thus, the effective non-Hermitian Hamiltonian [74] is

$$H_{eff} = H_{tot} + H_d - i\frac{\gamma_c}{2} a^\dagger a. \tag{22}$$

The excitation number is small when the rate of external laser driving is in the weak-driving regime $\eta/\gamma_c \ll 1$. So we can work within the few excitation number subspace spanned by the basis states $|0\rangle$, $|1\rangle$, $|2\rangle$, and $|3\rangle$ of the cavity field. The general state Equation (21) of the system can be simplified as

$$|\varphi(t)\rangle = \sum_{n=0}^{3}\sum_{m=0}^{\infty} C_{n,m,e}(t)|n\rangle|\tilde{m}(n)\rangle_e|e\rangle + \sum_{n=0}^{3}\sum_{m=0}^{\infty} C_{n,m,g}(t)|n\rangle|\tilde{m}(n)\rangle_g|g\rangle, \tag{23}$$

where $C_{n,m,e}$ and $C_{n,m,g}$ are probability amplitudes. According to the effective Hamiltonian H_{eff}, simplified wave function $|\varphi(t)\rangle$, and the Schrödinger equation, the equations of motion for the probability amplitudes are

$$\dot{C}_{0,m,e(g)}(t) = -iE_{0,m,e(g)}C_{0,m,e(g)}(t) - i\eta \sum_{m'=0}^{\infty} {}_{e(g)}\langle \tilde{m}(0)|\tilde{m'}(1)\rangle_{e(g)} C_{1,m',e(g)}(t), \tag{24}$$

$$\begin{aligned}\dot{C}_{1,m,e(g)}(t) = &-(\frac{\gamma_c}{2} + iE_{1,m,e(g)})C_{1,m,e(g)}(t) - i\eta \sum_{m'=0}^{\infty} {}_{e(g)}\langle \tilde{m}(1)|\tilde{m'}(0)\rangle_{e(g)} C_{0,m',e(g)}(t) \\ &-i\sqrt{2}\eta \sum_{m'=0}^{\infty} {}_{e(g)}\langle \tilde{m}(1)|\tilde{m'}(2)\rangle_{e(g)} C_{2,m',e(g)}(t),\end{aligned} \tag{25}$$

$$\begin{aligned}\dot{C}_{2,m,e(g)}(t) = &-(\gamma_c + iE_{2,m,e(g)})C_{2,m,e(g)}(t) - i\sqrt{2}\eta \sum_{m'=0}^{\infty} {}_{e(g)}\langle \tilde{m}(2)|\tilde{m'}(1)\rangle_{e(g)} C_{1,m',e(g)}(t) \\ &-i\sqrt{3}\eta \sum_{m'=0}^{\infty} {}_{e(g)}\langle \tilde{m}(2)|\tilde{m'}(3)\rangle_{e(g)} C_{3,m',e(g)}(t),\end{aligned} \tag{26}$$

$$\dot{C}_{3,m,e(g)}(t) = -(\frac{3\gamma_c}{2} + iE_{3,m,e(g)})C_{3,m,e(g)}(t) - i\sqrt{3}\eta \sum_{m'=0}^{\infty} {}_{e(g)}\langle \tilde{m}(3)|\tilde{m'}(2)\rangle_{e(g)} C_{2,m',e(g)}(t). \tag{27}$$

The weak external driving, with a driving rate which is much less than the cavity dissipation rate (i.e., $\eta \ll \gamma_c$), excites a few photon-states in the cavity. Thus, Equations (24)–(27) can be approximately solved when the higher-order terms in the zero-, one-, and two-photon probability amplitudes are discarded [23], i.e., dropping the second, third, and third terms in Equations (24), (25), and (26), respectively. We only keep parts of the same magnitude in Equations (24)–(27). Then, the approximate solution of Equations (24)–(27) are

$$C_{0,m,e(g)}(t) = C_{0,m,e(g)}(0)e^{-iE_{0,m,e(g)}t}, \tag{28}$$

$$C_{1,m,e(g)}(t) = -\eta \sum_{m'=0}^{\infty} \frac{{}_{e(g)}\langle \tilde{m}(1)|\tilde{m'}(0)\rangle_{e(g)} C_{0,m',e(g)}(0)e^{-iE_{0,m',e(g)}t}}{E_{1,m,e(g)} - E_{0,m',e(g)} - i\frac{\gamma_c}{2}}, \tag{29}$$

$$\begin{aligned}C_{2,m,e(g)}(t) = &\sqrt{2}\eta^2 \sum_{m',m''=0}^{\infty} \frac{{}_{e(g)}\langle \tilde{m}(2)|\tilde{m'}(1)\rangle_{e(g)}}{E_{2,m,e(g)} - E_{0,m'',e(g)} - i\gamma_c} \\ &\times \frac{{}_{e(g)}\langle \tilde{m'}(1)|\tilde{m''}(0)\rangle_{e(g)} C_{0,m'',e(g)}(0)e^{-iE_{0,m'',e(g)}t}}{E_{1,m',e(g)} - E_{0,m'',e(g)} - i\frac{\gamma_c}{2}},\end{aligned} \tag{30}$$

$$\begin{aligned}C_{3,m,e(g)}(t) = &-\sqrt{6}\eta^3 \sum_{m',m'',m'''=0}^{\infty} \frac{{}_{e(g)}\langle \tilde{m}(3)|\tilde{m'}(2)\rangle_{e(g)}}{E_{3,m,e(g)} - E_{0,m''',e(g)} - i\frac{3\gamma_c}{2}} \\ &\times \frac{{}_{e(g)}\langle \tilde{m'}(2)|\tilde{m''}(1)\rangle_{e(g)}}{E_{2,m',e(g)} - E_{0,m''',e(g)} - i\gamma_c} \times \frac{{}_{e(g)}\langle \tilde{m''}(1)|\tilde{m'''}(0)\rangle_{e(g)} C_{0,m''',e(g)}(0)e^{-iE_{0,m''',e(g)}t}}{E_{1,m'',e(g)} - E_{0,m''',e(g)} - i\frac{\gamma_c}{2}},\end{aligned} \tag{31}$$

where $C_{1,m,e(g)}(0) = C_{2,m,e(g)}(0) = C_{3,m,e(g)}(0) = 0$ is the initial situation for an initial empty cavity and $C_{0,m,e(g)}(0)$, $C_{0,m',e(g)}(0)$, $C_{0,m'',e(g)}(0)$, and $C_{0,m''',e(g)}(0)$ are determined by the initial state of the Bogoliubov mode and two-level impurity. We assume $\Delta n = n' - n$. The result of the Franck–Condon factors ${}_{e(g)}\langle \tilde{m'}(n')|\tilde{m}(n)\rangle_{e(g)}$ is

$$\langle m'|e^{\beta(\Delta n)(b^\dagger - b)}|m\rangle = \begin{cases} \sqrt{\frac{m'!}{m!}} e^{-\frac{[\beta(\Delta n)]^2}{2}} [-\beta(\Delta n)]^{m-m'} L_{m'}^{m-m'}\left([\beta(\Delta n)]^2\right), & m \geq m' \\ \sqrt{\frac{m!}{m'!}} e^{-\frac{[\beta(\Delta n)]^2}{2}} [\beta(\Delta n)]^{m'-m} L_{m}^{m'-m}\left([\beta(\Delta n)]^2\right), & m' > m \end{cases} \tag{32}$$

where $L_i^j(x)$ is the associated Laguerre polynomial, and $\beta = \sqrt{2}\lambda_{CB}(\cosh\zeta - \sinh\zeta)/(2\Omega_b + \lambda_s)$ is a system-dependent constant. We assume the Bogoliubov mode is in squeezing vacuum states, initially. Then, the probability amplitudes take the form $C_{0,m,e(g)}(0) = \delta_{0,m}C_{e(g)}$, where C_e and C_g are determined by the initial state of the two-level impurity. So far, the probability amplitude of the system wave function in the few-photon subspace can be approximately obtained

$$C_{0,m,e(g)}(t) = C_{e(g)}e^{-iE_{0,0,e(g)}t}, \tag{33}$$

$$C_{1,m,e(g)}(t) = -\eta\frac{\langle m|e^{\beta(b^\dagger - b)}|0\rangle C_{e(g)}e^{-iE_{0,0,e(g)}t}}{E_{1,m,e(g)} - E_{0,0,e(g)} - i\frac{\gamma_c}{2}}, \tag{34}$$

$$C_{2,m,e(g)}(t) = \sqrt{2}\eta^2\sum_{m'=0}^{\infty}\frac{\langle m|e^{\beta(b^\dagger - b)}|m'\rangle}{E_{2,m,e(g)} - E_{0,0,e(g)} - i\gamma_c} \times \frac{\langle m'|e^{\beta(b^\dagger - b)}|0\rangle C_{e(g)}e^{-iE_{0,0,e(g)}t}}{E_{1,m',e(g)} - E_{0,0,e(g)} - i\frac{\gamma_c}{2}}, \tag{35}$$

$$C_{3,m,e(g)}(t) = -\sqrt{6}\eta^3\sum_{m',m''=0}^{\infty}\frac{\langle m|e^{\beta(b^\dagger - b)}|m'\rangle}{E_{3,m,e(g)} - E_{0,0,e(g)} - i\frac{3\gamma_c}{2}} \times \frac{\langle m'|e^{\beta(b^\dagger - b)}|m''\rangle}{E_{2,m',e(g)} - E_{0,0,e(g)} - i\gamma_c} \times \frac{\langle m''|e^{\beta(b^\dagger - b)}|0\rangle C_{e(g)}e^{-iE_{0,0,e(g)}t}}{E_{1,m'',e(g)} - E_{0,0,e(g)} - i\frac{\gamma_c}{2}}. \tag{36}$$

The antibunching effects of the cavity field include single-photon, two-photon blockade, and non-standard photon blockade in our situation. For the same externally driven source, the anharmonicity of the cavity field energy level leads to a change in the probability of the cavity absorbing photons with the change in the number of photons in the cavity. The ideal single-photon blockade is that there is only one photon in the cavity, and the absorption of the previous photon will prevent subsequent photons from entering the cavity, i.e., the probability of finding two photons in the cavity is largely suppressed due to the energy restriction. Therefore, the correlation between intracavity photons and subsequent photons is absent. The condition for the single-photon blockade is the zero-time-delay normalized SOC function $g^{(2)}(0) < 1$ (i.e., $g^{(2)}(0) \to 0$ corresponds to complete single-photon blockade). Similarly, the two-photon blockade with two-photon bunching and three-photon antibunching requires the SOC and TOC to satisfy $g^{(2)}(0) \geq 1$ and $g^{(3)}(0) < 1$ [75,76]. The non-standard photon blockade is characterized by the SOC and TOC function satisfying the conditions $g^{(2)}(0) < 1 < g^{(3)}(0)$ [77,78], where the two-photon correlation is suppressed and the three-photon correlation is enhanced.

When the cavity field is in state Equation (23), the SOC and TOC function of single mode optical field in occupation number representation reads

$$g^{(2)}(0) = \frac{\langle a^\dagger a^\dagger aa\rangle}{\langle a^\dagger a\rangle^2} = \frac{2P_2}{(P_1 + 2P_2)^2}, \tag{37}$$

$$g^{(3)}(0) = \frac{\langle a^\dagger a^\dagger a^\dagger aaa\rangle}{\langle a^\dagger a\rangle^3} = \frac{6P_3}{(P_1 + 2P_2 + 3P_3)^2}, \tag{38}$$

where $P_i = \sum_{m=0}^{\infty}\left(|C_{i,m,e}(\infty)|^2 + |C_{i,m,g}(\infty)|^2\right)$ is the probabilities for finding i photons in the cavity. Based on Equation (33)–(36), the photon probabilities P_i $(i = 0, 1, 2, 3)$, SOC function $g^{(2)}(0)$, and TOC function $g^{(3)}(0)$ can be obtained.

3.2. The Manipulation of Single-Photon Blockade

The SOC function $g^{(2)}(0)$ shows that the photon statistics transits between super-Poissonian ($g^{(2)}(0) > 1$) and sub-Poissonian ($g^{(2)}(0) < 1$) distributions with the change of δ_a, which correspond to classical and non-classical effects, respectively. In particular, the dips in these curves correspond to the single-photon resonant driving cases. In such a case, a single photon can be resonantly excited into the cavity, but the probability of finding

two photons in the cavity is largely suppressed due to the energy restriction. This effect of the sub-Poissonian distributions is often referred to as single-photon blockade ($g^{(2)}(0) \ll 1$, i.e., a dip).

Figure 2 describes the effect of the initial state of impurity on the single-photon blockade in our hybrid quantum system. In Figure 2, we plot the SOC function $g^{(2)}(0)$ as a function of δ_a when the impurity initial state parameters C_g and C_e take various values. In Figure 2a, the initial state of impurity is ground ($C_g = 1$) or excited ($C_e = 1$) state, the corresponding left dip D_1 or right dip D_2 are both smaller than 0.1. When the initial state of impurity is a superposition state ($C_g = C_e = 1/\sqrt{2}$), the dips of D_3 and D_4 will appear simultaneously at the positions corresponding to dip D_1 and D_2, respectively, in Figure 2b. However, the minimum value of $g^{(2)}(0)$ of the dip D_3 and D_4 becomes larger than D_1 and D_2, respectively. Figure 2c also shows that the dips of $D_5(D_7)$ and $D_6(D_8)$ will appear simultaneously at the same positions. One can find that the value of dip $D_7(D_5)$ and $D_6(D_8)$ are both smaller (larger) than D_3 and D_4. The value of the left (right, relative to the point $\delta_a = 0.5$) dip will decrease as the probability amplitude of $C_g(C_e)$ increases. In general, the blockading range is larger when the initial state of impurity is a superposition state compared to when the initial state of the impurity is only a ground or excited state. Additionally, the single-photon blockade will be enhanced with the increase in the impurity initial state probability amplitude. At the same time, the position of the single-photon blockade does not change with the initial state of the impurity probability amplitude.

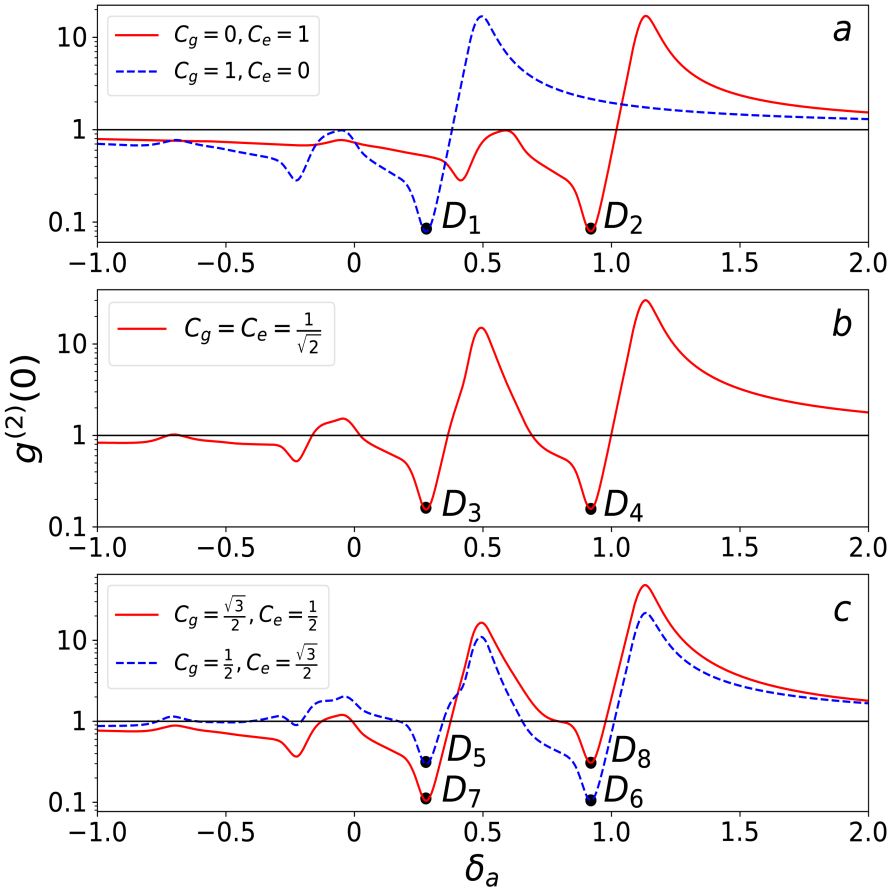

Figure 2. The equal-time SOC function $g^{(2)}(0)$ of the cavity field versus the driving detuning δ_a for various values of the impurity initial state parameters: (**a**) $C_g = 0, C_e = 1$ (red solid line), $C_g = 1, C_e = 0$ (blue dashed line), (**b**) $C_g = C_e = 1/\sqrt{2}$ (red solid line), and (**c**) $C_g = \sqrt{3}/2, C_e = 1/2$ (red solid line), $C_g = 1/2, C_e = \sqrt{3}/2$ (blue dashed line). Other parameters are $\lambda_s = 0.5$, $\Omega_b = 1, \omega_i' = 1, \lambda_{iC} = 0.08, \lambda_{CB} = \sqrt{2}/2, \lambda_{iB} = 1, \eta = 0.01, \gamma_c = 0.1$ in units of Ω_b.

The effect of the BEC internal interaction strength λ_s on the cavity single-photon blockade is plotted in Figure 3 within a certain parameter range. The situation of $\lambda_s > 0$ ($\lambda_s < 0$) indicates repulsive (attractive) interaction within the BEC [63]. In the attractive interaction ($\lambda_s < 0$) situation within the BEC, according to Figure 3a, the value of the left and right dip (relative to the point $\delta_a = 0.2$) decreases as the absolute value of λ_s increases ($D_1 > D_2 > D_3$ and $D_4 > D_5 > D_6$).

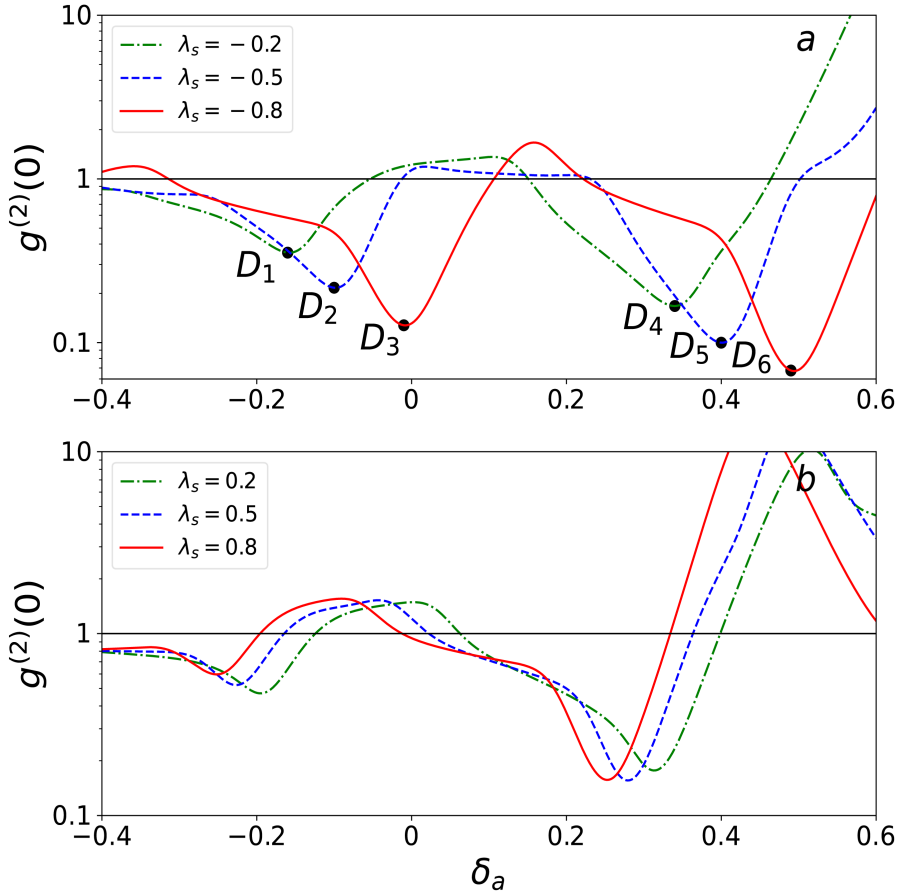

Figure 3. The equal-time SOC function $g^{(2)}(0)$ of the cavity field versus the driving detuning δ_a for various values of the BEC internal interaction strength λ_s: (**a**) $\lambda_s = -0.8$ (red solid line), $\lambda_s = -0.5$ (blue dashed line), $\lambda_s = -0.2$ (green dotdashed line) and (**b**) $\lambda_s = 0.8$ (red solid line), $\lambda_s = 0.5$ (blue dashed line), $\lambda_s = 0.2$ (green dotdashed line). Other parameters are $C_e = C_g = \sqrt{2}/2, \Omega_b = 1, \omega_i' = 1, \lambda_{iC} = 0.08, \lambda_{CB} = \sqrt{2}/2, \lambda_{iB} = 1, \eta = 0.01, \gamma_c = 0.1$ in units of Ω_b.

Additionally, one can find that the area enclosed by the curve of $g^2(0)$ and $g^2(0) = 1$ will increase with the increasing of the absolute value of λ_s, when moving to the right. In Figure 3b, if the value of repulsive interaction strength λ_s becomes larger, the value of $g^2(0)$ of the right dips is approximately invariant, but the left dips becomes greater. The minimum value of $g^2(0)$ of the left dips is approximately equal to 1, so the single-photon blockade is not obvious. The single-photon blockade in the left dips will also vanish if the value of λ_s continues to increase. Thus, the BEC internal interaction can enhance or weaken cavity single-photon blockade under certain conditions in our situation.

To further study the effect of the interaction induced by two-level impurity on the cavity single-photon blockade in the hybrid cavity–BEC quantum system, we plot $g^2(0)$ as a function of δ_a for different values of λ_{iB} and λ_{iC} in Figure 4. Comparing Figure 4a with Figure 4b, we find the minimum value of $g^2(0)$ is smaller than 0.1 at the dip near $\delta_a \approx 0.3$ in the blue dashed line of Figure 4a. Thus, the strong single-photon blockade ($g^2(0) \ll 1$) can be observed at $\lambda_{iB} = 0.2$. If the impurity–BEC interaction strength λ_{iB} is not equal to

0.2, the variation of interaction λ_{iB} will increase the value of $g^2(0)$ of the dip, compared with the situation $\lambda_{iB} = 0.2$. Thus, the single-photon blockade near but for $\lambda_{iB} = 0.2$ is weakened. On the whole, if the value of λ_{iB} is smaller than the half of the effective transition frequency ω_i', the impurity–BEC interaction has a weak effect on the single-photon blockade in Figure 4a. However, if the value of λ_{iB} becomes larger, the impurity–BEC interaction results in a new obvious right dip (relative to the point $\delta_a = 0.5$) in Figure 4b.

In the traditional radiation pressure type cavity–BEC system without impurity atom, single-photon blockade occurs only at a particular optical driving frequency under a certain condition. In Figure 4c, we demonstrate the fine-tuning of the impurity-cavity coupling parameter λ_{iC} on the cavity single-photon blockade. Figure 4d,e are enlargements of the left and right dip positions in Figure 4c. The coupling strength λ_{iC} can only move the position and has no effect on the value of each dip. This means that the single-photon blockade can be realized with optional frequencies by tuning the strength of impurity–cavity coupling. At the same time, one can use the coupling strength λ_{iC} to fine-tune the energy level of the cavity to make the single-photon blockade as strong as possible at a particular optical driving frequency.

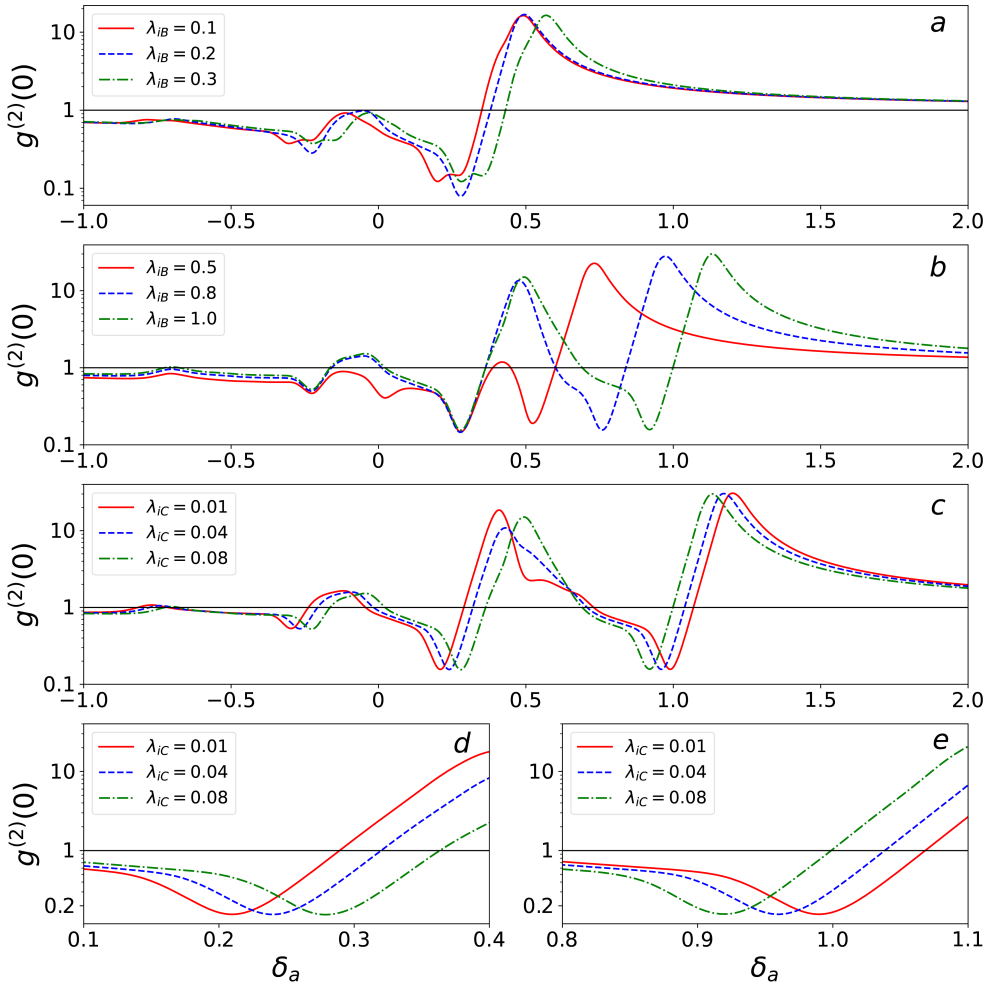

Figure 4. The equal-time SOC function $g^{(2)}(0)$ of the cavity field versus the driving detuning δ_a for various values of the impurity–BEC interaction strength λ_{iB} and impurity–cavity interaction strength λ_{iC}: (**a**) $\lambda_{iB} = 0.1$ (red solid line), $\lambda_{iB} = 0.2$ (blue dashed line), $\lambda_{iB} = 0.3$ (green dotdashed line), (**b**) $\lambda_{iB} = 0.5$ (red solid line), $\lambda_{iB} = 0.8$ (blue dashed line), $\lambda_{iB} = 1.0$ (green dotdashed line), and (**c**) $\lambda_{iC} = 0.01$ (red solid line), $\lambda_{iC} = 0.04$ (blue dashed line), $\lambda_{iC} = 0.08$ (green dotdashed line). Other parameters are $C_e = C_g = \sqrt{2}/2, \lambda_s = 0.5, \Omega_b = 1, \omega_i' = 1, \lambda_{CB} = \sqrt{2}/2, \eta = 0.01, \gamma_c = 0.1$, (**a**) $\lambda_{iC} = 0.08$, (**c**) $\lambda_{iB} = 1.0$ in units of Ω_b. (**d**,**e**) are enlargements of the left and right dip positions in (**c**).

3.3. The Manipulation of Two-Photon Blockade and Non-Standard Photon Blockade

The internal interaction of the system can prevent the system from absorbing the further photons when there are already two photons in the cavity, which is the two-photon blockade. That means the two-photon correlation will be enhanced, and the three-photon correlation will be suppressed. Thus, the two-photon blockade can be used to generate the non-classical photon pairs, which has potential for preparing the entangled photon sources. The two-photon blockade with two-photon bunching and three-photon antibunching can be obtained in our system. In order to study the manipulation of the two-photon blockade in our situation, we firstly introduce the criterion of the two-photon blockade, which is $g^{(2)}(0) > 1$ and $g^{(3)}(0) < 1$ [75,76,79]. The criterion of a strong two-photon blockade is $g^{(2)}(0) > 1$ and $g^{(3)}(0) < 0.01$ [80]. By using these criteria, we can study the effect of system parameter changes on the two-photon blockade distribution region in our situation.

The dependence of the zero-time-delay normalized SOC function $g^{(2)}(0)$ and TOC function $g^{(3)}(0)$ on the detuning δ_a are shown in Figure 5 for different impurity initial states. According to the two-photon blockade criterion, the two-photon blockade can be obtained when the impurity initial states are single states or superposition states, as displayed by the cyan areas in Figure 5. In Figure 5a or Figure 5b, the area of the two photon blockade is single when the initial state of the impurity is in the ground or excited state. However, the two-photon blockade region is enlarged when the impurity initial state is in the superposition state by comparing Figure 5a–c. The underlying physics of this phenomenon is attributed to the impurity initial state coherence, which can enhance the two-photon correlation of cavity.

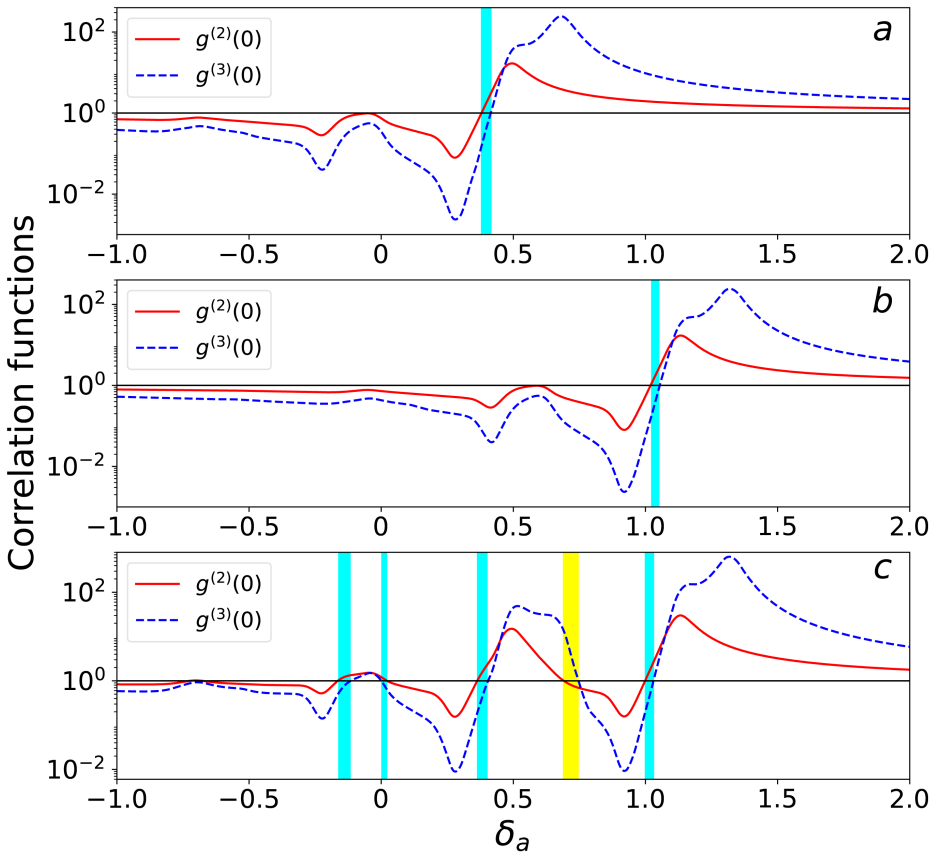

Figure 5. The equal-time SOC function $g^{(2)}(0)$ and TOC function $g^{(3)}(0)$ of the cavity field versus the driving detuning δ_a for various values of the impurity initial state parameters: (**a**) $C_e = 0, C_g = 1$, (**b**) $C_e = 1, C_g = 0$, and (**c**) $C_e = C_g = \sqrt{2}/2$. Other parameters are $\lambda_s = 0.5$, $\Omega_b = 1, \omega_i' = 1, \lambda_{iC} = 0.08, \lambda_{CB} = \sqrt{2}/2, \lambda_{iB} = 1, \eta = 0.01, \gamma_c = 0.1$ in units of Ω_b.

In addition to this trends, we also find the superbunching effect or dubbed the non-standard photon blockade in our system [76–78]. The yellow area in Figure 5c indicates that the SOC function $g^{(2)}(0)$ is less than 1 and the TOC function $g^{(3)}(0)$ is greater than 1. This corresponds to the two-photon correlation being suppressed and the three-photon correlation being enhanced, expressing preferential three-photon bunching. Comparing Figure 5a–c, one can find that the superbunching effect exists only when the impurity initial state is a superposition state. Thus, the initial coherence of impurity is favorable for the preparation of two-photon blockade and non-standard photon blockade.

In Figure 6, the correlation functions of $g^{(2)}(0)$ and $g^{(3)}(0)$ are shown in their dependence on the detuning δ_a for different impurity–BEC coupling strengths. As one can see, there are ranges of the detuning δ_a for which $g^{(2)}(0) > 1$ is accompanied by the additional condition for $g^{(3)}(0) < 1$ in cyan area, which implies the occurrence of the two-photon blockade. Comparing Figure 6a,b, the case of impurity–BEC coupling strength $\lambda_{iB} = 0.8$ has more cyan area than that of $\lambda_{iB} = 0.5$. However, according to Figure 6b,c, the ranges of the cyan area of the two-photon blockade have not changed significantly when all other parameters are the same except λ_{iB}. Moreover, the yellow areas in Figure 6b,c indicate non-standard photon blockade similar to the one in Figure 5c. Comparing Figure 6b,c, the range of detuning δ_a for realizing the non-standard photon blockade in impurity–BEC coupling strength $\lambda_{iB} = 1$ is wider to some extent than that of $\lambda_{iB} = 0.8$. Combining the above two points, the enhancement of the impurity–BEC interaction strength λ_{iB} in a certain range can manipulate the two-photon blockade and non-standard photon blockade.

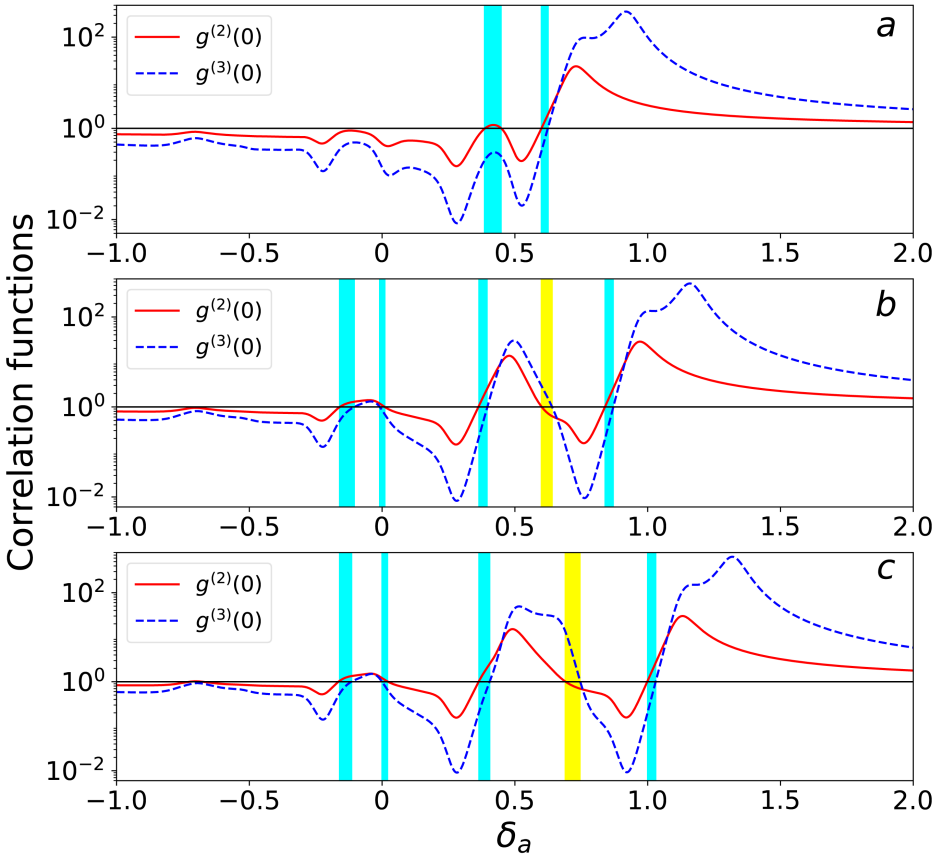

Figure 6. The equal-time SOC function $g^{(2)}(0)$ and TOC function $g^{(3)}(0)$ of the cavity field versus the driving detuning δ_a for various values of the impurity–BEC coupling strength: (**a**) $\lambda_{iB} = 0.5$, (**b**) $\lambda_{iB} = 0.8$, and (**c**) $\lambda_{iB} = 1$. Other parameters are $C_e = C_g = \sqrt{2}/2$ and $\lambda_s = 0.5$, $\Omega_b = 1, \omega_i' = 1, \lambda_{iC} = 0.08, \lambda_{CB} = \sqrt{2}/2, \eta = 0.01, \gamma_c = 0.1$ in units of Ω_b.

4. Discussion

The hybrid cavity–BEC system is composed of a two-level impurity atom and a cavity–BEC system with radiation pressure coupling. In spite of similarities between the two kinds of optomechanical systems (with a moving mirror and a BEC), the radiation pressure coupling in a cavity–BEC system is different from that in a bare optomechanical system. Firstly, the frequency of the BEC Bogoliubov mechanical mode is a controllable parameter in cavity–BEC systems [25,34]. However, the frequency of the mechanical mode of the moving mirror is a fixed parameter in a bare optomechanical system. Secondly, the radiation pressure coupling strength can be increased to strong coupling by increasing the number of atoms [28,29]. As we know, the radiation pressure coupling is a key factor in the non-linear structure of the cavity field energy level [24]. Thus, we believe that studying the optical antibunching effects with cavity–BEC systems have greater advantages than a bare optomechanical systems.

We add a two-level impurity atom to the cavity–BEC systems, which will complicate the composition of the systems. The advantage that comes with this is that we have more ways to manipulate the system. Hui Wang et al. studied the tuning of photon blockade by a two-level system in hybrid optomechanical devices. They found that the photon blockade and tunneling can be significantly changed by the transition frequency of the two-level system and the coupling strength between the two-level system and the mechanical resonator [81]; however, they did not consider the coupling between the impurity atoms and the cavity field. We found that the dispersion interaction between a two-level impurity and the cavity field also has the effects of manipulating the photon antibunching effects in our situation.

Finally, there has been a great deal of work investigating two-photon blockade and multi-photon blockade in a quantum system. Adam Miranowicz et al. demonstrated how various photon blockades can be identified by analyzing photon-number correlations, coherence and entropic properties, Wigner functions, and spectra of squeezing [82]. Qian Bin et al. found that the two-photon blockade can be obtained even when the strong system dissipation is included in a cascaded cavity–quantum-electrodynamics system [76]. Anna K-K et al. showed that two-photon blockade and other non-standard types of photon blockade can be generated in a driven harmonic cavity, which only couples with a non-linear (i.e., squeezed) reservoir [78]. Here, we have simultaneously studied the single-photon blockade, two-photon blockade, and superbunching effect in a hybrid cavity–BEC system. This has contributed to the study of the diversity of quantum systems and the integration of quantum resources.

5. Conclusions

In this paper, we first introduce the hybrid cavity–BEC quantum system, which consists of a Fabry–Perot cavity, cigar-shaped BEC, and a two-level impurity atom. Here, the effective Hamiltonian of the hybrid cavity–BEC quantum system is proposed under certain approximations. On this basis, the effective Hamiltonian of our system can be successively diagonalized by using the displacement operator and the squeezing operator. Secondly, we have studied the steady-state photon antibunching effects of the hybrid cavity–BEC quantum system. In our situation, the cavity is weakly excited by a monochromatic laser field. Thus, we can treat the driving term as a perturbation. Then, the approximate analytical expression of the SOC and TOC function for the cavity photons can be obtained by truncating the Hilbert space of the cavity.

The single-photon blockade, two-photon blockade, and non-standard photon blockade can be observed in our system. We find that these antibunching effects of the cavity are significantly affected within a certain parameter range by the internal interaction of BEC and an impurity when the cavity–impurity interaction is under large detuning conditions. The single-photon blockade can be enhanced with the increasing of the impurity initial state probability amplitude and internal interaction strength of BEC. The increase in BEC–impurity interaction can induce the new blockade dips and resonant peaks for the SOC

function. Moreover, the position of the new blockade dips and resonant peaks can be tuned if we change the BEC–impurity interaction strength. However, the cavity–impurity interaction can only move the position and has no effect on the value, as well as quantity, of blockade dips in the dispersive limit.

The two-photon blockade with two-photon bunching and three-photon antibunching also can be observed in our hybrid quantum system when the cavity dissipation is taken into account. Furthermore, the range of frequency for realizing the two-photon blockade effect in our system can be expanded with the enhancement of the coherence of the impurity initial state and BEC–impurity interaction. In particular, in the same parameters, we have also observed the non-standard photon blockade or superbunching effect, where the probability of measuring two photons at the same time is suppressed. Simultaneously, the probability of obtaining three photons is enhanced. That is, our study may provide an indirect manipulation scheme for the antibunching effect of the cavity field in the hybrid cavity–BEC quantum system under certain approximations. The study of multiple types of antibunching effects will advance the development of preparing single photon sources and photon pairs and have potential applications in quantum information science.

Author Contributions: The contributions of author Z.L. are Conceptualization, methodology, validation and formal analysis. The contributions of author W.L. are software and data curation. All authors have read and agreed to the published version of the manuscript.

Funding: This research was supported by the National Natural Science Foundation of China (grant number 12205092).

Institutional Review Board Statement: Not applicable.

Informed Consent Statement: Not applicable.

Data Availability Statement: This study did not report any data.

Conflicts of Interest: The authors declare no conflict of interest.

Appendix A. Diagonalization of the Hamiltonian H_{tot}

Appendix A.1. The First Step of Diagonalization

The optical field excitation number and the impurity population are conservative in H_{tot}. The Bogoliubov mode has the form of driving fields and quadratically coupling. Thus, in the first step of diagonalization, we use the like displacement operator

$$D(\alpha a^\dagger a) = \exp\Big[\alpha a^\dagger a(b^\dagger - b)\Big], \tag{A1}$$

where the operator α is defined as

$$\alpha = \frac{\sqrt{2}\lambda_{CB}a^\dagger a + \lambda_{iB}(\sigma_z + 1)}{(2\Omega_b + \lambda_s)a^\dagger a}. \tag{A2}$$

Using the form of the like displacement operator given in Equation (A1) and the Baker–Campbell–Hausdorff formula, we have

$$b' = D(\alpha a^\dagger a)bD^\dagger(\alpha a^\dagger a) = b - \alpha a^\dagger a, \tag{A3}$$

$$b'^\dagger = D(\alpha a^\dagger a)b^\dagger D^\dagger(\alpha a^\dagger a) = b^\dagger - \alpha a^\dagger a. \tag{A4}$$

The Hamiltonian H_{tot} can be transformed into the following form

$$\begin{aligned} H'_{tot} &= D(\alpha a^\dagger a)H_{tot}D^\dagger(\alpha a^\dagger a) \\ &= \delta_a a^\dagger a + \Omega_b b'^\dagger b' + \frac{\omega'_i}{2}\sigma_z + \lambda_{iC}a^\dagger a\sigma_z + \frac{1}{4}\lambda_s(b'^2 + b'^{\dagger 2}) \\ &\quad + \frac{1}{2}\Big[\sqrt{2}\lambda_{CB}a^\dagger a + \lambda_{iB}(\sigma_z + 1)\Big](b' + b'^\dagger), \end{aligned} \tag{A5}$$

Substituting the Equation (A3) and Equation (A4) into the Equation (A5), the Hamiltonian H'_{tot} will be rewritten as

$$H'_{tot} = \delta_a a^\dagger a + \Omega_b b^\dagger b + \frac{\omega'_i}{2}\sigma_z + \lambda_{iC} a^\dagger a \sigma_z + \frac{1}{4}\lambda_s (b^2 + b^{\dagger 2}) - \left(\Omega_b + \frac{1}{2}\lambda_s\right)\alpha^2 (a^\dagger a)^2, \quad \text{(A6)}$$

Appendix A.2. The Second Step of Diagonalization

The Hamiltonian H'_{tot} is diagonal in terms of the creation and annihilation operators of the optical field, while it is not diagonal in terms of the operators of the Bogoliubov mode due to the presence of quadratically coupling term. Thus, we can select the squeezing operator to diagonalize the Hamiltonian H'_{tot}. The definition of squeezing operator is

$$S(\zeta) = \exp\left(\frac{1}{2}\zeta (b^2 - b^{\dagger 2})\right), \quad \text{(A7)}$$

where ζ is the squeezing parameter. The effect of this squeezing unitary transformation on the operators b and $b^\dagger$ will obtain the following operators

$$b'' = S(\zeta) b S^\dagger(\zeta) = b\cosh\zeta + b^\dagger \sinh\zeta, \quad \text{(A8)}$$

$$b''^\dagger = S(\zeta) b^\dagger S^\dagger(\zeta) = b\sinh\zeta + b^\dagger \cos\zeta. \quad \text{(A9)}$$

Then, applying the squeezing unitary transformation Equations (A8) and (A9) to Equation (A6), the Hamiltonian of H'_{tot} becomes

$$\begin{aligned} H''_{tot} &= S(\zeta) H'_{tot} S^\dagger(\zeta) \\ &= \delta_a a^\dagger a + \Omega_b b''^\dagger b'' + \frac{\omega'_i}{2}\sigma_z + \lambda_{iC} a^\dagger a \sigma_z + \frac{1}{4}\lambda_s (b''^2 + b''^{\dagger 2}) \\ &\quad - \left(\Omega_b + \frac{1}{2}\lambda_s\right)\alpha^2 (a^\dagger a)^2. \end{aligned} \quad \text{(A10)}$$

Finally, the Hamiltonian H''_{tot} will have the diagonalized form in terms of the operators b and $b^\dagger$ as follows:

$$H''_{tot} = \delta_a a^\dagger a + \Omega'_b b^\dagger b + \frac{\omega'_i}{2}\sigma_z + \lambda_{iC} a^\dagger a \sigma_z - \left(\Omega_b + \frac{1}{2}\lambda_s\right)\alpha^2 (a^\dagger a)^2, \quad \text{(A11)}$$

where the effective Bogoliubov mode frequency Ω'_b and squeezing parameter ζ need to satisfy the following system of algebraic equations:

$$\Omega_b\left(\cosh^2\zeta + \sinh^2\zeta\right) + \lambda_s \cosh\zeta \sinh\zeta = \Omega'_b, \quad \text{(A12)}$$

$$\Omega_b \cosh\zeta \sinh\zeta + \frac{1}{4}\lambda_s\left(\cosh^2\zeta + \sinh^2\zeta\right) = 0, \quad \text{(A13)}$$

$$\cosh^2\zeta - \sinh^2\zeta = 1. \quad \text{(A14)}$$

Solving the above system of algebraic equations, the effective Bogoliubov mode frequency Ω'_b and squeezing parameter ζ read

$$\Omega'_b = \sqrt{\left(4\omega_R + \frac{1}{2}\lambda_s\right)\left(4\omega_R + \frac{3}{2}\lambda_s\right)}, \quad \text{(A15)}$$

$$\cosh\zeta = \frac{1}{\sqrt{2}}\sqrt{\frac{\Omega_b}{\Omega'_b} + 1}. \quad \text{(A16)}$$

Note that this diagonalization method has been used to research the squeezed states of BEC in cavity [83].

References

1. Ishizaki, K.; Noda, S. Manipulation of photons at the surface of three-dimensional photonic crystals. *Nature* **2009**, *460*, 367–370. [CrossRef] [PubMed]
2. Kim, Y.B.; Cho, J.W.; Lee, Y.J.; Bae, D.; Kim, S.K. High-index-contrast photonic structures: A versatile platform for photon manipulation. *Light. Sci. Appl.* **2022**, *11*, 1–16. [CrossRef] [PubMed]
3. Murray, C.R.; Pohl, T. Coherent photon manipulation in interacting atomic ensem-bles. *Phys. Rev. X* **2017**, *7*, 031007.
4. Zhou, M.G.; Cao, X.Y.; Lu, Y.S.; Wang, Y.; Bao, Y.; Jia, Z.Y.; Fu, Y.; Yin, H.L.; Chen, Z.B. Experimental quantum advantage with quantum coupon collector. *Research* **2022**, *2022*, 9798679. [CrossRef] [PubMed]
5. Liu, W.B.; Li, C.L.; Xie, Y.M.; Weng, C.X.; Gu, J.; Cao, X.Y.; Lu, Y.S.; Li, B.H.; Yin, H.L.; Chen, Z.B. Homodyne detection quadrature phase shift keying continuous-variable quantum key dis-tribution with high excess noise tolerance. *PRX Quantum* **2021**, *2*, 040334. [CrossRef]
6. Xie, Y.M.; Lu, Y.S.; Weng, C.X.; Cao, X.Y.; Jia, Z.Y.; Bao, Y.; Wang, Y.; Fu, Y.; Yin, H.L.; Chen, Z.B. Breaking the rate-loss bound of quantum key distribution with asynchronous two-photon interference. *PRX Quantum* **2022**, *3*, 020315. [CrossRef]
7. Brune, M.; Haroche, S.; Raimond, J.M.; Davidovich, L.; Zagury, N. Manipulation of photons in a cavity by dispersive atom-field coupling: Quantum-nondemolition measurements and genera-tion of "Schrödinger cat" states. *Phys. Rev. A* **1992**, *45*, 5193. [CrossRef]
8. Lu, W.; Zhai, C.; Tang, S. Measuring the pth-Order Correlation Function of Light Field via Two-Level Atoms. *Photonics* **2022**, *9*, 727. [CrossRef]
9. Paul, H. Photon antibunching. *Rev. Mod. Phys.* **1982**, *54*, 1061. [CrossRef]
10. Kimble, H.J.; Dagenais, M. Photon antibunching in resonance fluorescence. *Phys. Rev. Lett.* **1977**, *39*, 691. [CrossRef]
11. Wu, Z.; Shen, S.; Li, J.; Wu, Y. Photon antibunching as a probe of trajectory information of individual neutral atoms traversing an optical cavity. *Phys. Rev. A* **2021**, *104*, 053710. [CrossRef]
12. Steindl, P.; Snijders, H.; Westra, G.; Hissink, E.; Iakovlev, K.; Polla, S.; Frey, J.A.; Norman, J.; Gossard, A.C.; Bowers, J.E.; et al. Artificial coherent states of light by multiphoton interfer-ence in a single-photon stream. *Phys. Rev. Lett.* **2021**, *126*, 143601. [CrossRef]
13. Muñoz-Matutano, G.; Johnsson, M.; Martínez-Pastor, J.; Rivas Góngora, D.; Seravalli, L.; Trevisi, G.; Frigeri, P.; Volz, T.; Gurioli, M. All optical switching of a sin-gle photon stream by excitonic depletion. *Commun. Phys.* **2020**, *3*, 29. [CrossRef]
14. Lounis, B.; Orrit, M. Single-photon sources. *Rep. Prog. Phys.* **2005**, *68*, 1129. [CrossRef]
15. Yuan, Z.; Kardynal, B.E.; Stevenson, R.M.; Shields, A.J.; Lobo, C.J.; Cooper, K.; Beattie, N.S.; Ritchie, D.A.; Pepper, M. Electrically driven single-photon source. *Science* **2002**, *295*, 102–105. [CrossRef]
16. Takeuchi, S. Recent progress in single-photon and entangled-photon generation and applications. *Jpn. J. Appl. Phys.* **2014**, *53*, 030101. [CrossRef]
17. Ma, X.; Fung, C.H.F.; Lo, H.K. Quantum key distribution with entangled photon sources. *Phys. Rev. A* **2007**, *76*, 012307. [CrossRef]
18. Neumann, S.P.; Scheidl, T.; Selimovic, M.; Pivoluska, M.; Liu, B.; Bohmann, M.; Ursin, R. Model for optimizing quantum key distribution with continuous-wave pumped entangled-photon sources. *Phys. Rev. A* **2021**, *104*, 022406. [CrossRef]
19. Hoffman, A.J.; Srinivasan, S.J.; Schmidt, S.; Spietz, L.; Aumentado, J.; Türeci, H.E.; Houck, A.A.; Dispersive photon blockade in a superconducting circuit. *Phys. Rev. Lett.* **2011**, *107*, 053602. [CrossRef]
20. Liu, Y.X.; Xu, X.W.; Miranowicz, A.; Nori, F. From blockade to transparency: Control-lable photon transmission through a circuit-QED system. *Phys. Rev. A* **2014**, *89*, 043818. [CrossRef]
21. Birnbaum, K.M.; Boca, A.; Miller, R.; Boozer, A.D.; Northup, T.E.; Kimble, H.J. Photon blockade in an optical cavity with one trapped atom. *Nature* **2005**, *436*, 87–90. [CrossRef] [PubMed]
22. Lang, C.; Bozyigit, D.; Eichler, C.; Steffen, L.; Fink, J.M.; Abdumalikov, A.A., Jr.; Baur, M.; Filipp, S.; da Silva, M.P.; Blais, A.; et al. Observation of resonant photon blockade at micro-wave frequencies using correlation function measurements. *Phys. Rev. Lett.* **2011**, *106*, 243601. [CrossRef] [PubMed]
23. Liao, J.Q.; Nori, F. Photon blockade in quadratically coupled optomechanical systems. *Phys. Rev. A* **2013**, *88*, 023853. [CrossRef]
24. Rabl, P. Photon blockade effect in optomechanical systems. *Phys. Rev. Lett.* **2011**, *107*, 063601. [CrossRef] [PubMed]
25. Brennecke, F.; Ritter, S.; Donner, T.; Esslinger, T. Cavity optomechanics with a Bose-Einstein condensate. *Science* **2008**, *322*, 235–238. [CrossRef]
26. Robb, G.R.M.; Tesio, E.; Oppo, G.L.; Firth, W.J.; Ackemann, T.; Bonifacio, R. Quantum threshold for optomechanical self-structuring in a Bose-Einstein condensate. *Phys. Rev. Lett.* **2015**, *114*, 173903. [CrossRef]
27. Murch, K.W.; Moore, K.L.; Gupta, S.; Stamper-Kurn, D.M. Observation of quan-tum-measurement backaction with an ultracold atomic gas. *Nat. Phys.* **2008**, *4*, 561–564. [CrossRef]
28. Chauhan, A.K.; Biswas, A. Motion-induced enhancement of Rabi coupling between atomic ensembles in cavity optomechanics. *Phys. Rev. A* **2017**, *95*, 023813. [CrossRef]
29. Szirmai, G.; Nagy, D.; Domokos, P. Quantum noise of a Bose-Einstein condensate in an optical cavity, correlations, and entanglement. *Phys. Rev. A* **2010**, *81*, 043639. [CrossRef]
30. Dalafi, A.; Naderi, M.H. Controlling steady-state bipartite entanglement and quadra-ture squeezing in a membrane-in-the-middle optomechanical system with two Bose-Einstein condensates. *Phys. Rev. A* **2017**, *96*, 033631. [CrossRef]

31. Motazedifard, A.; Dalafi, A.; Naderi, M.H. Ultraprecision quantum sensing and measurement based on nonlinear hybrid optomechanical systems containing ultracold atoms or atomic Bose-Einstein condensate. *AVS Quantum Sci.* **2021**, *3*, 024701. [CrossRef]
32. Dalafi, A.; Naderi, M.H. Dispersive interaction of a Bose-Einstein condensate with a movable mirror of an optomechanical cavity in the presence of laser phase noise. *Phys. Rev. A* **2016**, *94*, 063636. [CrossRef]
33. Motazedifard, A.; Dalafi, A.; Naderi, M.H.; Roknizadeh, R. Strong quadrature squeezing and quantum amplification in a coupled Bose-Einstein condensate-optomechanical cavity based on parametric modulation. *Ann. Phys.* **2019**, *405*, 202–219. [CrossRef]
34. Dalafi, A.; Naderi, M.H.; Soltanolkotabi, M.; Barzanjeh, S. Nonlinear effects of atomic collisions on the optomechanical properties of a Bose-Einstein condensate in an optical cavity. *Phys. Rev. A* **2013**, *87*, 013417. [CrossRef]
35. Balewski, J.B.; Krupp, A.T.; Gaj, A.; Peter, D.; Büchler, H.P.; Löw, R.; Hofferberth, S.; Pfau, T. Coupling a single electron to a Bose-Einstein condensate. *Nature* **2013**, *502*, 664–667. [CrossRef]
36. Ng, H.T.; Bose, S. Single-atom-aided probe of the decoherence of a Bose-Einstein con-densate. *Phys. Rev. A* **2008**, *78*, 023610. [CrossRef]
37. Wang, J.; Gacesa, M.; Côté, R. Rydberg electrons in a Bose-Einstein condensate. *Phys. Rev. Lett.* **2015**, *114*, 243003. [CrossRef]
38. Schmidt, R.; Sadeghpour, H.R.; Demler, E. Mesoscopic Rydberg impurity in an atomic quantum gas. *Phys. Rev. Lett.* **2016**, *116*, 105302. [CrossRef]
39. Heidemann, R.; Raitzsch, U.; Bendkowsky, V.; Butscher, B.; Löw, R.; Pfau, T. Rydberg excitation of Bose-Einstein condensates. *Phys. Rev. Lett.* **2008**, *100*, 033601. [CrossRef]
40. Mukherjee, R.; Ates, C.; Li, W.; Wüster, S. Phase-imprinting of Bose-Einstein condensates with Rydberg impurities. *Phys. Rev. Lett.* **2015**, *115*, 040401. [CrossRef]
41. Johnson, T.H.; Yuan, Y.; Bao, W.; Clark, S.R.; Foot, C.; Jaksch, D. Hubbard model for atomic impurities bound by the vortex lattice of a rotating bose-einstein condensate. *Phys. Rev. Lett.* **2016**, *116*, 240402. [CrossRef] [PubMed]
42. Li, Z.; Lu, W. Transient and Fast Generation of Bose-Einstein-Condensate Macroscopic Quantum Superposition States via Impurity Catalysing. *Photonics* **2022**, *9*, 622. [CrossRef]
43. Song, Y.J.; Kuang, L.M. Controlling Decoherence Speed Limit of a Single Impurity Atom in a Bose-Einstein-Condensate Reservoir. *Ann. Der Phys.* **2019**, *531*, 1800423. [CrossRef]
44. Yuan, J.B.; Xing, H.J.; Kuang, L.M.; Yi, S. Quantum non-Markovian reservoirs of atomic condensates engineered via dipolar interactions. *Phys. Rev. A* **2017**, *95*, 033610. [CrossRef]
45. Yuan, J.B.; Kuang, L.M. Quantum-discord amplification induced by a quantum phase transition via a cavity-Bose-Einstein-condensate system. *Phys. Rev. A* **2013**, *87*, 024101. [CrossRef]
46. Li, Z.; Kuang, L.M. Controlling quantum coherence of a two-component Bose-Einstein condensate via an impurity atom. *Quantum Inf. Process.* **2020**, *19*, 188. [CrossRef]
47. Li, Z.; Han, Y.; Kuang, L.M. Complementarity between micro-micro and micro-macro entanglement in a Bose-Einstein condensate with two Rydberg impurities. *Commun. Theor. Phys.* **2020**, *72*, 025101. [CrossRef]
48. Lu, W.; Zhai, C.; Liu, Y.; Song, Y.; Yuan, J.; Tang, S. Berry Phase of Two Impurity Qubits as a Signature of Dicke Quantum Phase Transition. *Photonics* **2022**, *9*, 844. [CrossRef]
49. Lu, W.; Zhai, C.;Liu, Y.; Song, Y.; Yuan, J.; Li, S.; Tang, S. Quantum Speed-Up Induced by the Quantum Phase Transition in a Nonlinear Dicke Model with Two Impurity Qubits. *Symmetry* **2022**, *14*, 2653. [CrossRef]
50. Tan, Q.S.; Xie, Q.T.; Kuang, L.M. Effects of dipolar interactions on the sensitivity of nonlinear spinor-BEC interterometry. *Sci. Rep.* **2018**, *8*, 3218. [CrossRef]
51. Tan, Q.S.; Yuan, J.B.; Jin, G.R.; Kuang, L.M. Near-Heisenberg-limited parameter es-timation precision by a dipolar-Bose-gas reservoir engineering. *Phys. Rev. A* **2017**, *96*, 063614. [CrossRef]
52. Mehboudi, M.; Lampo, A.; Charalambous, C.; Correa, L.A.; García-March, M. Á.; Lewenstein, M. Using polarons for sub-nk quantum nondemolition thermometry in a bose-einstein condensate. *Phys. Rev. Lett.* **2019**, *122*, 030403. [CrossRef]
53. Bruderer, M.; Jaksch, D. Probing BEC phase fluctuations with atomic quantum dots. *New J. Phys.* **2006**, *8*, 87. [CrossRef]
54. Zhao, C.; Li, X.; Chao, S.; Peng, R.; Li, C.; Zhou, L.; Simultaneous blockade of a photon, phonon, and magnon induced by a two-level atom. *Phys. Rev. A* **2020**, *101*, 063838. [CrossRef]
55. Alotaibi, M.F.; Khalil, E.M.; Abdel-Khalek, S.; Abd-Rabbou, M.Y.; Omri, M. Effects of the vibrating graphene membrane and the driven classical field on an atomic system coupled to a cavity field. *Results Phys.* **2021**, *31*, 105012. [CrossRef]
56. Alotiabi, M.F.; Khalil, E.M.; Abd-Rabbou, M.Y. Dynamics of an atomic system associated with a cavity-optomechanical system. *Results Phys.* **2022**, *37*, 105540. [CrossRef]
57. Anderson, W.R.; Veale, J.R.; Gallagher, T.F. Resonant dipole-dipole energy transfer in a nearly frozen Rydberg gas. *Phys. Rev. Lett.* **1998**, *80*, 249. [CrossRef]
58. Weimer, H.; Löw, R.; Pfau, T.; Büchler, H.P. Quantum critical behavior in strongly interacting Rydberg gases. *Phys. Rev. Lett.* **2008**, *101*, 250601. [CrossRef]
59. Morsch, O.; Oberthaler, M. Dynamics of Bose-Einstein condensates in optical lattices. *Rev. Mod. Phys.* **2006**, *78*, 179. [CrossRef]
60. Maschler, C.; Ritsch, H. Quantum motion of laser-driven atoms in a cavity field. *Opt. Commun.* **2004**, *243*, 145–155. [CrossRef]
61. Motazedifard, A.; Dalafi, A.; Bemani, F.; Naderi, M.H. Force sensing in hybrid Bose-Einstein-condensate optomechanics based on parametric amplification. *Phys. Rev. A* **2019**, *100*, 023815. [CrossRef]

62. Timmermans, E.; Tommasini, P.; Hussein, M.; Kerman, A. Feshbach resonanc-es in atomic Bose-Einstein condensates. *Phys. Rep.* **1999**, *315*, 199–230. [CrossRef]
63. Bloch, I.; Dalibard, J.; Zwerger, W. Many-body physics with ultracold gases. *Rev. Mod. Phys.* **2008**, *80*, 885. [CrossRef]
64. Maschler, C.; Ritsch, H. Cold atom dynamics in a quantum optical lattice potential. *Phys. Rev. Lett.* **2005**, *95*, 260401. [CrossRef] [PubMed]
65. Treutlein, P.; Steinmetz, T.; Colombe, Y.; Lev, B.; Hommelhoff, P.; Reichel, J.; Greiner, M.; Mandel, O.; Widera, A.; Rom, T.; et al. Quantum information processing in optical lattices and magnetic microtraps. *Fortschritte Phys. Prog. Phys.* **2006**, *54*, 702–718. [CrossRef]
66. Savage, C.M.; Braunstein, S.L.; Walls, D.F. Macroscopic quantum superpositions by means of single-atom dispersion. *Opt. Lett.* **1990**, *15*, 628–630. [CrossRef]
67. Gerry, C.; Knight, P.; Knight, P.L. *Introductory Quantum Optics*; Cambridge University Press: Cambridge, UK, 2005.
68. Agarwal, G.S.; Puri, R.R.; Singh, R.P. Atomic Schrödinger cat states. *Phys. Rev. A* **1997**, *56*, 2249. [CrossRef]
69. Zheng, S.B.; Guo, G.C. Efficient scheme for two-atom entanglement and quantum in-formation processing in cavity QED. *Phys. Rev. Lett.* **2000**, *85*, 2392. [CrossRef]
70. Xing, Y.; Qi, L.; Zhao, X.; Lü, Z.; Liu, S.; Zhang, S.; Wang, H.F. Quantum transport in a one-dimensional quasicrystal with mobility edges. *Phys. Rev. A* **2022**, *105*, 032443. [CrossRef]
71. Liu, S.; Chen, Y.H.; Wang, Y.; Kang, Y.H.; Shi, Z.C.; Song, J.; Xia, Y. Generation of cat states by a weak parametric drive and a transitionless tracking algorithm. *Phys. Rev. A* **2022**, *106*, 042430. [CrossRef]
72. Li, K.Z.; Xu, G.F. Robust population transfer of spin states by geometric formalism. *Phys. Rev. A* **2022**, *105*, 052433. [CrossRef]
73. Nagy, D.; Domokos, P.; Vukics, A.; Ritsch, H. Nonlinear quantum dynamics of two BEC modes dispersively coupled by an optical cavity. *Eur. Phys. J. D* **2009**, *55*, 659–668. [CrossRef]
74. James, D.F.; Jerke, J. Effective Hamiltonian theory and its applications in quantum information. *Can. J. Phys.* **2007**, *85*, 625–632. [CrossRef]
75. Hamsen, C.; Tolazzi, K.N.; Wilk, T.; Rempe, G. Two-photon blockade in an at-om-driven cavity QED system. *Phys. Rev. Lett.* **2017**, *118*, 133604. [CrossRef]
76. Bin, Q.; Lü, X.Y.; Bin, S.W.; Wu, Y. Two-photon blockade in a cascaded cavi-ty-quantum-electrodynamics system. *Phys. Rev. A* **2018**, *98*, 043858. [CrossRef]
77. Radulaski, M.; Fischer, K.A.; Lagoudakis, K.G.; Zhang, J.L.; Vučković, J. Photon blockade in two-emitter-cavity systems. *Phys. Rev. A* **2017**, *96*, 011801. [CrossRef]
78. Kowalewska -Kudłaszyk, A.; Abo, S.I.; Chimczak, G.; Peřina, J., Jr.; Nori, F.; Miranowicz, A. Two-photon blockade and photon-induced tunneling generated by squeezing. *Phys. Rev. A* **2019**, *100*, 053857. [CrossRef]
79. Zhai, C.; Huang, R.; Jing, H.; Kuang, L.M. Mechanical switch of photon blockade and photon-induced tunneling. *Opt. Express* **2019**, *27*, 27649–27662. [CrossRef]
80. Hou, K.; Zhang, Z.; Zhu, C.; Yang, Y. Enhancement of the two-photon blockade effect via Van der Waals interaction. *Front. Phys.* **2022**, *10*, 979427. [CrossRef]
81. Wang, H.; Gu, X.; Liu, Y.X.; Miranowicz, A.; Nori, F. Tunable photon blockade in a hybrid system consisting of an optomechanical device coupled to a two-level system. *Phys. Rev. A* **2015**, *92*, 033806. [CrossRef]
82. Miranowicz, A.; Paprzycka, M.; Liu, Y.X.; Bajer, J.; Nori, F. Two-photon and three-photon blockades in driven nonlinear systems. *Phys. Rev. A* **2013**, *87*, 023809. [CrossRef]
83. Dalafi, A.; Naderi, M.H.; Soltanolkotabi, M. Squeezed-state generation via atomic collisions in a Bose-Einstein condensate inside an optical cavity. *J. Mod. Opt.* **2014**, *61*, 1387–1397. [CrossRef]